ChemistrySelect

Research Article
doi.org/10.1002/slct.202400178

Chemistry Europe
European Chemical Societies Publishing

www.chemistryselect.org

Synthesis of β-Truxinate via [2+2] Cycloaddition of Methyl 4-Nitrocinnamate: Kinetic Study of its Isomerization with DBU.

José Daniel Bahena-Martínez,[a] Roberto Flores,[b] Blanca Eda Domínguez-Mendoza,[a] Luis Gabriel Hernández-Vázquez,[a] Eusebio Juaristi,[c, d] and Jaime Escalante*[a]

This work concerns the isomerization of the product obtained by dimerization of methyl 4-nitrocinnamate. Subsequent isomerization was performed using 1,8-diazabicyclo[5.4.0]undec-7-ene (DBU) as a base to obtain the corresponding ζ- and δ-truxinate derivatives. The process was monitored by ^{1}H NMR spectroscopy in different deuterated solvents with a wide range of dielectric constants, acetonitrile-d_3, acetone-d_6, tetrahydrofuran-d_8, and benzene-d_6. Each solvent was found to have a distinct influence on the reaction's rate constant k, with acetone-d_6 yielding the highest ratio of ζ-truxinate derivative. Kinetic analysis of the reaction provided valuable information about the mechanism involved in the isomerization process.

Introduction

Truxinic and truxillic acids are constitutional isomers of cyclobutane-derived dicarboxylic acids, which differ in their relative configuration (Figure 1).[1]

Various types of natural products containing the truxinic or truxillic core have been isolated.[2–6] These include alkaloids, flavonoids, iridoids, sugars, and amino acids, among others.[7] In this regard, it has been reported that their derivatives isolated from natural sources frequently exhibit biological activity, such as anti-inflammatory, neuroprotective, anticancer, antidiabetic, and inhibitor of CYP34 A enzymatic activity.[8–12]

The most plausible manner by which the truxinic and truxillic cycloadducts are formed in nature is *via* [2+2] cycloadditions. Indeed, the cyclic compound are sometimes isolated together with the corresponding monomers. In this regard, Yuan et al.[3] reported that various configurational isomers of the cycloadducts are present in *Ginkgo biloba* leaves with different stereochemistry, presumably arising from [2+2] cycloaddition reactions (Figure 2).

ζ-Truxinates are less frequently found in natural products compared to α-truxilates and δ-truxinates, and few reports are

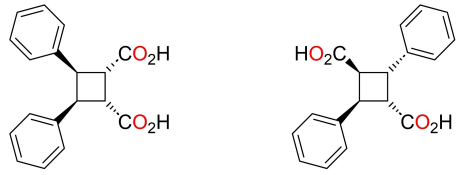

β-Truxinic acid α-Truxillic acid

Figure 1. Structure of β-truxinic and α-truxillic acids.

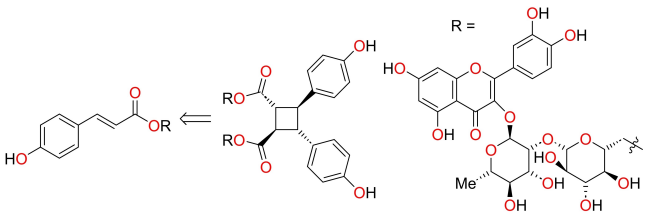

δ-Truxinate
Antineuroinflammatory activity

Figure 2. δ-Truxinate derivative found in Ginkgo biloba leaves and its unsaturated precursor.

available with regard to their synthesis or isolation from natural products.[7] For example, Nakamura reported the synthesis of ζ-truxinic acid in 0.56% yield by means of ultraviolet light irradiation of *trans*-cinnamic acid in micellar solutions.[13] In addition, Galindo and Miranda revealed the synthesis of ζ-truxinic acid derivatives by dimerization of vinyl cinnamate substrates using photosensitizers, with remarkable yields of up to 16%.[14]

In the present work, we report that the diastereoselective synthesis of ζ- and δ-truxinate derivatives can be accomplished by isomerization of the β-truxinate cycloadduct (synthesized from the dimerization of methyl 4-nitrocinnamate) using DBU as base. These experiments were conducted in deuterated solvents and monitored by ^{1}H NMR spectroscopy in order to derive the reaction's rate constants. In the following, relative to

[a] BSc. J. D. Bahena-Martínez, Dr. B. E. Domínguez-Mendoza, Dr. L. G. Hernández-Vázquez, Prof. J. Escalante
Centro de Investigaciones Químicas-IICBA, Universidad Autónoma del Estado de Morelos, Cuernavaca, Av. Universidad 1001, C.P. 62210, México
E-mail: jaime@uaem.mx

[b] Dr. R. Flores
Facultad de Ciencias Químicas e Ingeniería, Universidad Autónoma del Estado de Morelos, Cuernavaca, Av. Universidad 1001, C.P. 62210, México

[c] Prof. E. Juaristi
Centro de Investigación y de Estudios Avanzados, Av. Instituto Politécnico Nacional 2508, 07360 Ciudad de México, Mexico

[d] Prof. E. Juaristi
El Colegio Nacional, Luis González Obregón 23, Centro Histórico, 06020 Ciudad de México, Mexico

Supporting information for this article is available on the WWW under https://doi.org/10.1002/slct.202400178

the carbonyl group as reference, regioisomers are named as *cis*, *trans*, *trans* (*rctt*-**3a**); *cis*, *cis*, *trans* (*rcct*-**3b**) and *trans*, *cis*, *trans* (*rtct*-**3c**).[15]

Results and Discussion

Experimental section

In order to carry out the kinetic study of the isomerization of β-truxinate, *meso* cycloadduct *rctt*-**3a** was first synthesized (Scheme 1). The synthetic route begins with a Knoevenagel reaction between 4-nitrobenzaldehyde and malonic acid to give 4-nitrocinnamic acid **1**, as a white solid with a melting point of 294–296 °C, obtained in 92% yield.[16,17] Esterification of acid **1** was then achieved with quantitave yield using thionyl chloride and methanol. Cinnamate methyl ester **2** was isolated as a white solid with mp 161–164 °C, coinciding with reported value.[18] Thereafter, [2+2] solvent-free cycloaddition of **2** was realized in a Rayonet apparatus over 15 h. Cycloadduct *rctt*-**3a** was obtained as a white solid with a mp = 128–130 °C in 51% yield, and characterized by ^{1}H and ^{13}C NMR spectroscopy showing coincidence with Golfmann *et al.*.[19]

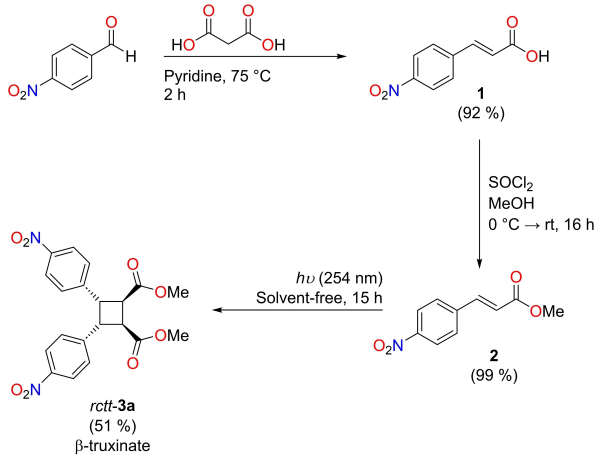

Scheme 1. Synthesis of cycloadduct β-truxinate rctt-**3a**.

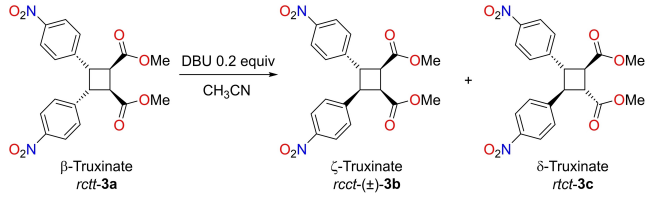

Scheme 2. Isomerization process for β-truxinate rctt-**3a**.

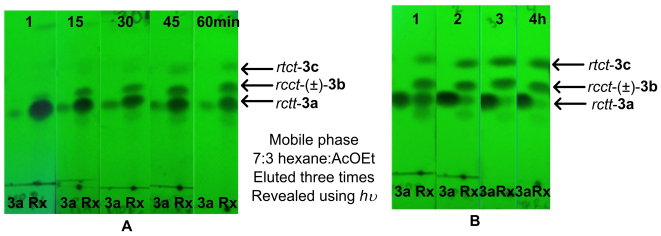

Figure 3. TLC Monitoring of rctt-**3a** isomerization. **A**) at room temperature and **B**) at 55 °C.

In order to find the best conditions for the isomerization process, additional experiments were carried out in 196 μL of acetonitrile using 0.2 equiv. of 1,8-diazabicyclo[5.4.0]undec-7-ene (DBU) as the base and at room temperature (Scheme 2).

As can be observed from Figure 3A formation of product *rcct*-(±)-**3b** (spectroscopic data coinciding with reported in literature[20]) is detected after one minute of reaction time, and its concentration increases as the reaction proceeds. The formation of *rtct*-**3c** (spectroscopic data coinciding with reported in literature[19]) is much slower, it only occurred after 45 minutes eventually reaching the same concentration as that of *rcct*-(±)-**3b**. When the reaction was completed, product purification afforded only 24% of *rcct*-(±)-**3b** and 50% of *rtct*-**3c**.

On the other hand, to increase the reaction's conversion, the temperature was raised to 55 °C and concentration was increased by using only 0.6 mL of solvent. In this experiment, after one hour of reaction (monitored by TLC), there was still unreacted compound *rctt*-**3a** present, together with a considerable amount of the products *rcct*-(±)-**3b** and *rtct*-**3c**. It is worth mentioning that TLC monitor (Figure 3B) also shows that the reaction continued after one hour.

The β-→ζ-→δ-truxinate isomerization process was then followed by ^{1}H NMR spectroscopy in a Bruker spectrometer (500 MHz). Four deuterated solvents of different polarity were chosen as reaction medium, acetonitrile (CD_3CN, ε = 37.5), acetone [$(CD_3)_2CO$, ε = 20.7], tetrahydrofuran (THF-d_8, ε = 7.6), and benzene, (C_6D_6, ε = 2.3).

Kinetic Isomerization in Deuterated Solvents

With the purpose of determining the ratio of the products in the reaction mixture, the appropriate signals for each isomeric structure were identified (See Supporting Information). For each kinetic measurement, the following general procedure was followed: 80 mM solution of *rctt*-**3a** was placed in a 3 mm resonance tube, 0.2 equiv. of DBU was added and the temperature was increased to 55 °C (t = 0) for CD_3CN, THF-d_8, and benzene-d_6. In the case of acetone-d_6 T = 45 °C was used. The progress of the reaction was followed at different time intervals.

a) Deuterated Acetonitrile

Kinetic studies were first carried out in deuterated acetonitrile. Figure 4 shows the ^{1}H NMR spectra recorded 30-minutes time intervals. By integrating the area under the curves, the ratio for each stereoisomer was determined (Table 1).

As it can be seen in Table 1, the yield of β-truxinate *rctt*-**3a** reaches 4.2% at 180 min (Entry 7), while ζ-truxinate *rcct*-(±)-**3b** and δ-truxinate *rtct*-**3c** are formed in nearly 50% each. Entry 4 in Table 1 shows that the concentration of *rcct*-(±)-**3b** initially reaches a maximum and subsequently decreases as the reaction proceeds.

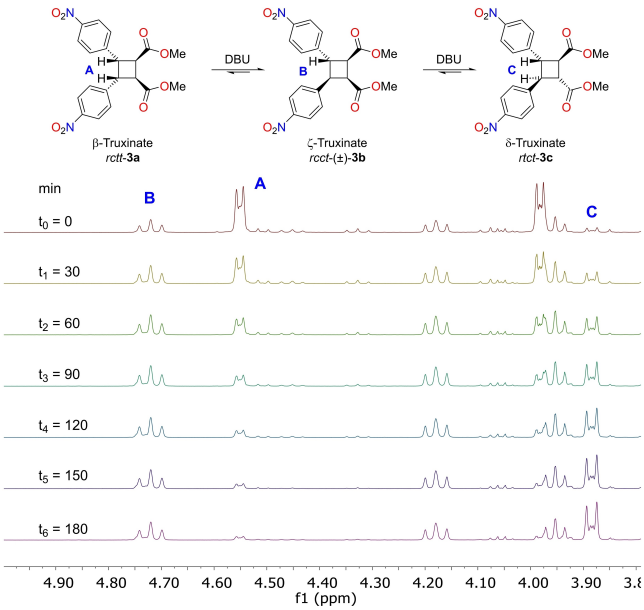

Figure 4. ^{1}H NMR isomerization kinetics in CD_3CN at 55 °C for rctt-**3a**.

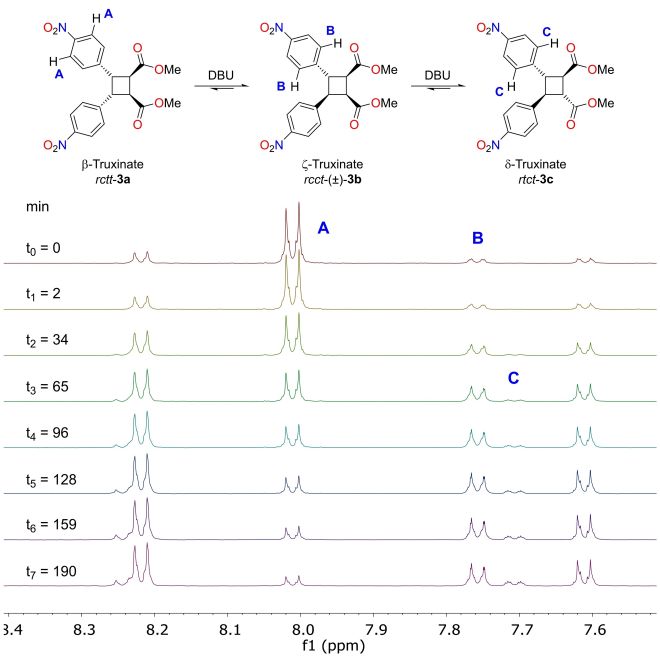

Figure 5. ^{1}H NMR isomerization kinetics in $(CD_3)_2CO$ at 45 °C for rctt-**3a**.

Table 1. Ratios observed by ^{1}H NMR in CD_3CN at 55 °C for truxinate derivatives.

Entry	Time (min)	*rctt*-**3a** (%)	*rcct*-(±)-**3b** (%)	*rtct*-**3c** (%)
1	0	63.49	31.75	4.76
2	30	37.71	48.66	13.63
3	60	23.22	54.64	22.13
4	90	14.45	56.66	28.90
5	120	9.14	55.40	35.46
6	150	6.10	53.05	40.85
7	180	4.23	49.75	46.02

Table 2. Relative ratios of truxinate derivatives observed by ^{1}H NMR in $(CD_3)_2CO$ at 45 °C.

Entry	Time (min)	*rctt*-**3a** (%)	*rcct*-(±)-**3b** (%)	*rtct*-**3c** (%)
1	0	81.30	18.70	0.00
2	2	79.68	20.32	0.00
3	34	58.14	39.83	2.03
4	65	42.74	53.42	3.85
5	96	32.87	61.79	5.34
6	128	24.62	68.31	7.08
7	159	19.09	71.89	9.02
8	190	14.92	74.15	10.93

b) Deuterated Acetone

As consequence of the anisotropic effect of deuterated acetone, the methine signals for the three stereoisomeric compounds appear overlapped. Therefore, it was necessary to use the signals of the aromatic ring as references for the quantification (Figure 5). The corresponding ratios obtained are collected in Table 2.

As can be seen in Table 2, the transformation of starting material *rctt*-**3a** is slower in comparison with the speed of reaction in deuterated acetonitrile. ζ-Truxinate *rcct*-(±)-**3b** can be obtained with higher yield (74.1 % in Entry 8), since *rcct*-(±)-**3b**→*rtct*-**3c** rate transformation is almost 4 times slower than of acetonitrile as solvent.

c) Deuterated Tetrahydrofuran

The kinetic study was then carried out in deuterated THF. As it was the case with acetone, the signals for the aromatic protons were used as reference to determine the stereoisomer ratios. The spectra for this kinetic analysis are shown in Figure 6 and the corresponding isomeric ratios are presented in Table 3.

As it can be seen from entry 8 in Table 3, the concentration of *rctt*-**3a** remains high (25 %) throughout the process. The

Table 3. Isomeric ratios observed by ^{1}H NMR in THF-d_8 at 55 °C for truxinate derivatives.

Entry	Time (min)	*rctt*-**3a** (%)	*rcct*-(±)-**3b** (%)	*rtct*-**3c** (%)
1	0	83.86	15.93	0.21
2	2	82.99	17.01	0.21
3	33	66.78	32.39	0.83
4	65	54.57	43.93	1.50
5	96	44.84	52.69	2.47
6	127	36.33	60.31	3.36
7	159	30.12	65.66	4.22
8	190	24.97	70.04	4.99

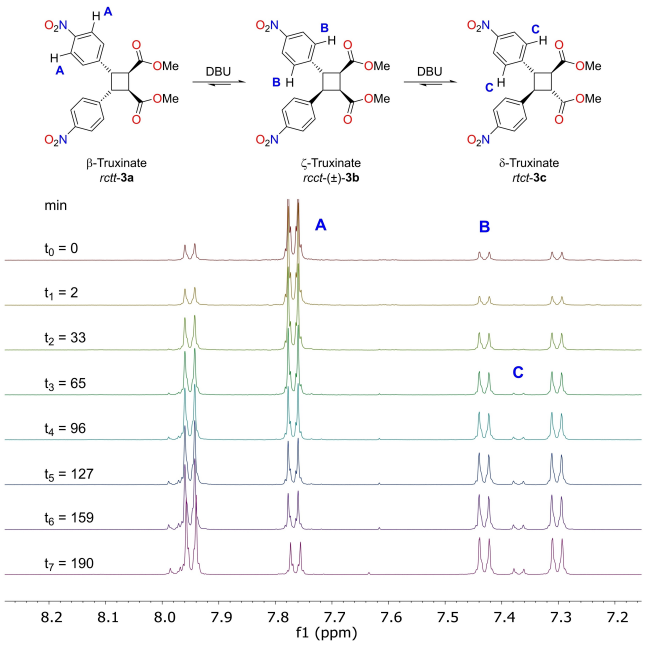

Figure 6. ^{1}H NMR isomerization kinetics in THF-d_8 at 55 °C for rctt-**3 a**.

relative ratio of *rcct*-(±)-**3 b** is only slightly lower than that observed in acetone (70.0 %), while the participation of *rtct*-**3 c** decreases even more in this solvent, down to 5 %.

d) Deuterated Benzene

The final kinetic study was carried out in deuterated benzene. For the determination of the stereoisomer ratios, the methine signals of the cycloadduct were used (Figure 7). As it can be noticed from Table 4, the rate constants for the formation of *rcct*-(±)-**3 b** and *rtct*-**3 c** are even lower than those in the other solvents, reaching for ζ-truxinate only 51.3 % yield over 191 min (Entry 8). It can also be noted that the *rtct*-**3 c** ratio remains essentially unchanged throughout the reaction.

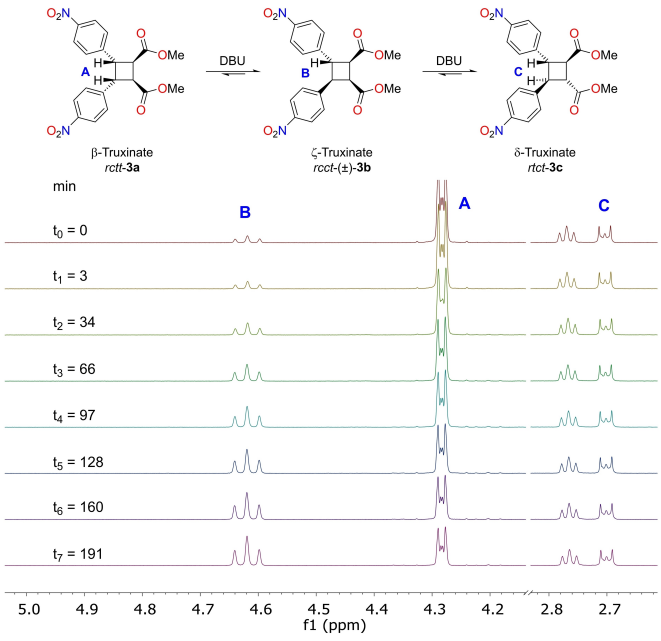

Figure 7. ^{1}H NMR isomerization kinetics in C_6D_6 at 55 °C for rctt-**3 a**.

Kinetic Model

From the experimental results, it is concluded that the reaction mechanism consists of two steps **A**→**B**→**C**. If one assumed that the reactions under consideration are unimolecular elementary, the resulting reaction rate equations can be expressed as follows:

$$\frac{dC_A}{dt} = -k_1 \cdot C_A$$

$$\frac{dC_B}{dt} = k_1 \cdot C_A - k_2 \cdot C_B$$

$$\frac{dC_C}{dt} = k_2 \cdot C_B$$

Using the separation of variables method,[21] the equation for the disappearance of **A** takes the form:

$$\ln\left(\frac{C_{A_0}}{C_A}\right) = k_1 \cdot t$$

In this manner, the value of k_1 for the various experimental runs of the isomerization of β-truxinate *rctt*-**3 a** can be estimated by solving a linear regression.

On the other hand, by solving the system of differential equations one obtained:

$$C_B = \frac{k_1 \cdot C_{A_0}}{k_2 - k_1} \cdot \left[e^{-k_1 \cdot t} - e^{-k_2 \cdot t}\right] + C_{B_0} \cdot e^{-k_2 \cdot t}$$

In this way, the calculation of k_2 is done iteratively, adopting varying values of k_2 until the objective function is minimized:

Table 4. Isomeric ratios observed by ^{1}H NMR in C_6D_6 at 55 °C for truxinate derivatives.

Entry	Time (min)	*rctt*-**3 a** (%)	*rcct*-(±)-**3 b** (%)	*rtct*-**3 c** (%)
1	0	75.41	10.81	13.78
2	3	74.31	11.98	13.71
3	34	65.17	20.86	13.97
4	66	57.08	28.90	14.02
5	97	49.55	36.30	14.16
6	128	43.82	41.93	14.26
7	160	38.44	47.17	14.39
8	191	34.10	51.28	14.62

$$\Phi = \sum \left(C_B^{exp} - C_B^{cal}\right)^2$$

Table 5. Calculated values for k_1 and k_2 in used deuterated solvents.

Solvent	k_1 (min^{-1})[a]	k_2 (min^{-1})[a]	Dielectric constant
CD_3CN	151	46	37.5
$(CD_3)_2CO$	90	10	20.7
THF-d_8	64	5	7.6
C_6D_6	42	1	2.3

[a]Expressed in 1×10^{-4} units.

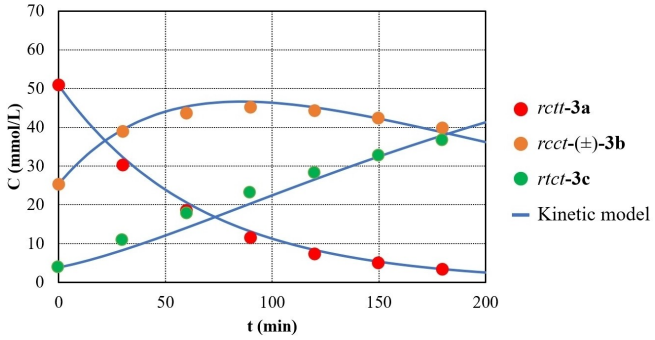

Figure 8. Experimental rctt-**3a**, rcct-(±)-**3b** and rtct-**3c** concentrations vs kinetic model (CD_3CN at 55 °C).

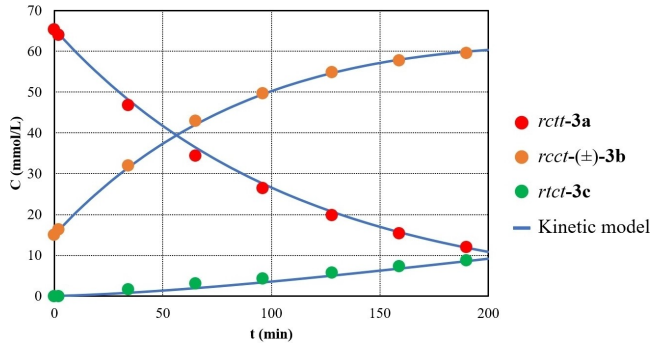

Figure 9. Experimental rctt-**3a**, rcct-(±)-**3b** and rtct-**3c** concentrations vs kinetic model [$(CD_3)_2CO$ at 45 °C].

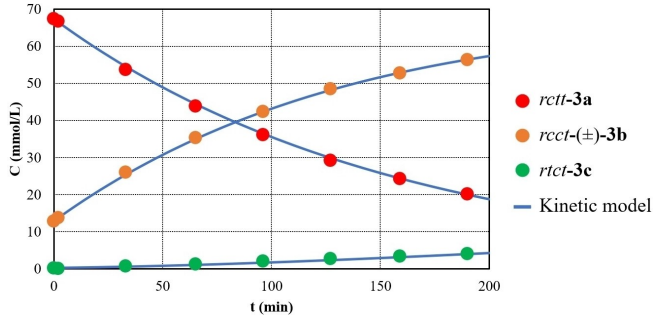

Figure 10. Experimental rctt-**3a**, rcct-(±)-**3b** and rtct-**3c** concentrations vs. kinetic model (THF-d_8 at 55 °C).

These calculations can be performed with a numerical optimization method, for example the Golden Section Method, or with the SOLVER function in Microsoft Excel.[22]

Table 5 shows the values obtained for k_1 and k_2 in the solvents where the isomerization reaction was studied, and Figures 8–11 show the necessary adjustment with respect to the experimental values.

Proposed Mechanistic Formation of Stereoisomers 3 b and 3 c

With the data gathered by ^{1}H NMR spectroscopic monitoring and the corresponding *k* values that were calculated, a reaction mechanism for the formation of both truxinate derivatives is proposed (Figure 12). This reaction mechanism is supported by

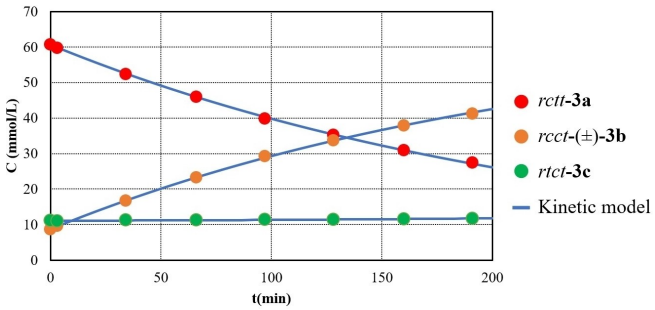

Figure 11. Experimental rctt-**3a**, rcct-(±)-**3b** and rtct-**3c** concentrations vs. kinetic model (C_6D_6 at 55 °C).

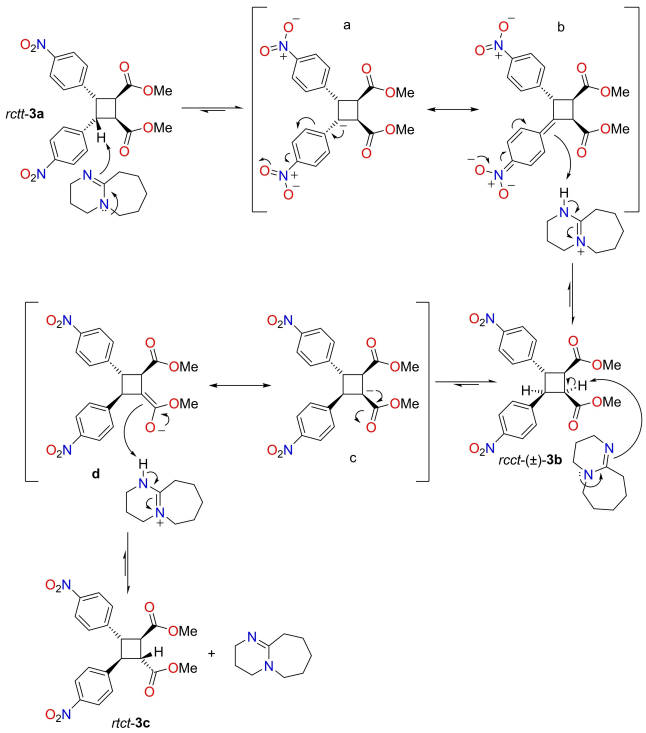

Figure 12. Proposed reaction mechanism for the formation of derivatives rcct-(±)-**3b** and rtct-**3c.**

the fact that the isomerization reaction is faster with increased acidity of the benzylic protons by the $-NO_2$ substituent in *para* position ($pK_a = 22.1$)[23] compared to the α protons to the carbonyl group ($pK_a = 25.6$).[24]

According to this proposal, the first step consists in a deprotonation of the benzylic proton by DBU and stabilization of the negative charge by the nitro group through the aromatic ring. In this way, the configuration of the stereogenic carbon is lost as a double bond is generated. Subsequently, the protonation of that carbon takes place preferentially on the face opposite to the two carboxylic groups to generate ζ-truxinate *rcct*-(±)-**3 b**. From the generated stereoisomer, formation of the enolate occurs by deprotonation of the carbon adjacent to the carbonyl group. Finally, protonation of the enolate takes place preferably on the face opposite to the carboxylic group to yield *rtct*-**3 c.**

The proposed reaction mechanism is in line with the general trend in rate constants induced by solvent polarity,[25] that is, protonation and deprotonation of molecules occurs faster as solvent polarity increases. This is reflected in the directly proportional relationship between dielectric strength and reaction rate constants, as shown in Figure 13.

Reports of solvent and substituent effects on the *Z*→*E* isomerization process for azobenzenes, which takes place via formation of a dipolar intermediate,[25] have shown that higher isomerization rate is observed when the polarity of the solvent is increased. Furthermore, according to the Hughes-Ingol rules, an increase in the polarity of the solvent, results in an increase of the reaction rate constant for those reactions where the charge density is higher in the activated complex than in the reactant molecule,[26] which fits well with the β-truxinate isomerization process reported herein.

The isomerization process *rctt*-**3 a**→*rcct*-(±)-**3 b**→*rtct*-**3 c** is favored by the releasing of the steric effect on the cyclobutane ring. This is achieved by switching from having adjacent groups oriented on the same side (*rctt*-**3 a**) to having them alternately (*rtct*-**3 c**). This was verified by isolating product ζ-Truxinate (*rcct*-(±)-**3 b**) and then carrying out the isomerization reaction (Scheme 3).

As can be observed from TLC at different time reactions (Figure 14), δ-truxinate (*rtct*-(±)-**3 c**) was detected after 1 h, and its concentration gradually increased until 7 h. It is noteworthy that β-truxinate *rctt*-**3 a** was not formed. This behaviour indicates that steric hindrance might be guiding the process since *rctt*-**3 a** is not formed from *rcct*-(±)-**3 b.**

Additionally, kinetics was carried out in CD_3CN as described in "Kinetic isomerization" (Figure 15). As can be observed only *rtct*-(±)-**3 c** was formed. The concentrations of isomers *rcct*-(±)-**3 b** and *rtct*-(±)-**3 c** are shown Table 6 and the trend can be observed in Figure 16.

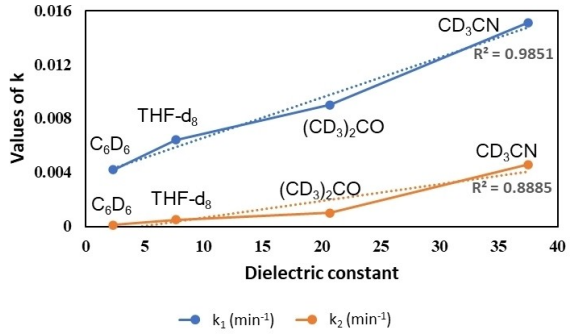

Figure 13. Values of k vs. solvent dielectric constant.

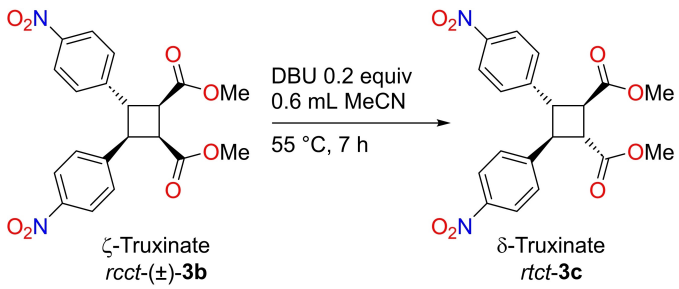

Scheme 3. Isomerization process for ζ-truxinate rcct-(±)-**3 b.**

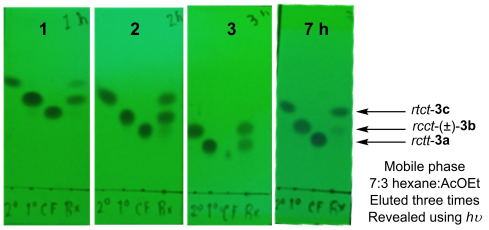

Figure 14. TLC Monitoring of rcct-(±)-**3 b** isomerization at 55 °C until 7 h.

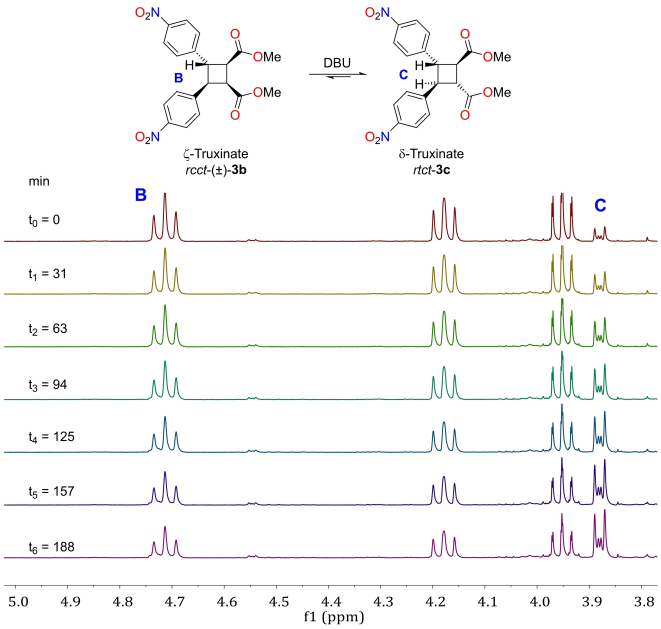

Figure 15. ^{1}H NMR isomerization kinetics starting from rcct-(±)-**3 b** in CD_3CN at 55 °C.

Table 6. Ratios observed by ^{1}H NMR in CD_3CN at 55 °C for truxinates rcct-(±)-**3 b** and rtct-**3 c** derivatives.

Entry	Time (min)	*rcct*-(±)-**3 b** (%)	*rtct*-**3 c** (%)
1	0	90.50	9.50
2	31	84.39	15.61
3	63	78.74	21.26
4	94	73.80	26.20
5	125	69.44	30.56
6	157	65.79	34.21
7	188	62.11	37.89

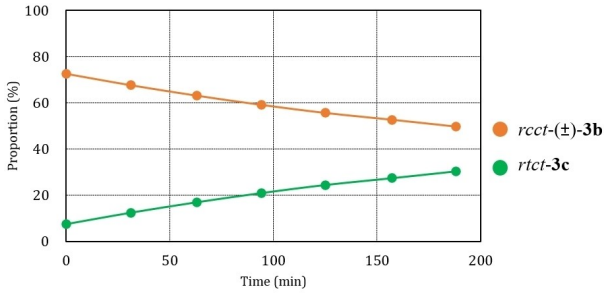

Figure 16. Experimental rcct-(±)-**3 b** and rtct-**3 c** concentrations in CD_3CN at 55 °C.

Conclusions

A novel, convenient method for the isomerization of β-truxinate *rctt*-**3 a** into ζ- and δ-truxinates *rcct*-(±)-**3 b** and *rtct*-**3 c**, is reported. This isomerization process was monitored by ^{1}H NMR in different deuterated solvents. As can be seen from the experimental data, the more polar the solvent, the higher the rate constant. The observed reaction rate constants show a linear relationship between *k* values and solvent dielectric constant, which favours the predominant formation of ζ- or δ-truxinate by appropriate selection of the solvent employed in the isomerization process.

Supporting Information

The Supporting information contains experimental procedures and spectroscopic characterization of compounds.

Acknowledgements

We would like to thank CONAHCYT for financial support (Project No. CB2019/610262). J. D. B.-M. thanks CONAHCYT for post-graduate scholarship with number 812421.

Conflict of Interests

The authors declare no conflict of interest.

Keywords: β-Truxinate · ζ-Truxinate · δ-Truxinate · DBU · Kinetic Isomerization

[1] Z. Rappoport, J. F. Liebman, Eds., *The Chemistry of Cyclobutanes*, Wiley, Hoboken, NJ, **2005**. ISBN 0-470-86400-1.
[2] G. Ablikim, K. Bobakulov, J. Li, N. Yadikar, H. A. Aisa, *Nat. Prod. Res.* **2021**, *35*, 2526–2534. DOI: 10.1080/14786419.2019.1684283.
[3] X. Yuan, Y. Liu, H. Zhao, L. Men, C. He, Y. Qiu, Q. Yu, K. Li, L. Qi, D. Chen, *Phytochemistry* **2021**, *181*, 112572. DOI: 10.1016/j.phytochem.2020.112572.
[4] J. Li, L.-H. Tan, H. Zou, Z.-X. Zou, H.-P. Long, W.-X. Wang, P.-S. Xu, L.-F. Liu, K.-P. Xu, G.-S. Tan, *J. Nat. Prod.* **2020**, *83*, 216–222. DOI: 10.1021/acs.jnatprod.9b00470.
[5] F. Zálešák, D. J.-Y. D. Bon, J. Pospíšil, *Pharmacol. Res.* **2019**, *146*, 104284. DOI: 10.1016/j.phrs.2019.104284.
[6] X. Yuan, L. Lin, X. Zhang, S. Deng, *Phytochem. Lett.* **2014**, *7*, 137–142. DOI: 10.1016/j.phytol.2013.11.003.
[7] X. Yuan, L. Men, Y. Liu, Y. Qiu, C. He, W. Huang, *J. Holistic Integrative Pharm.* **2020**, *1*, 48–69. DOI: 10.1016/S2707-3688(23)00039-0.
[8] G.-L. Ma, J. Xiong, G.-X. Yang, L.-L. Pan, C.-L. Hu, W. Wang, H. Fan, Q.-H. Zhao, H.-Y. Zhang, J.-F. Hu, *J. Nat. Prod.* **2016**, *79*, 1354–1364. DOI: 10.1021/acs.jnatprod.6b00061.
[9] I. S. Aljančić, I. Vučković, M. Jadranin, M. Pešić, I. Đorđević, A. Podolski-Renić, S. Stojković, N. Menković, V. E. Vajs, S. M. Milosavljević, *Phytochemistry* **2014**, *98*, 190–196. DOI: 10.1016/j.phytochem.2013.11.025.
[10] Y. Liu, X. Zhang, N. Kelsang, G. Tu, D. Kong, J. Lu, Y. Zhang, H. Liang, P. Tu, Q. Zhang, *J. Nat. Prod.* **2018**, *81*, 307–315. DOI: 10.1021/acs.jnatprod.7b00736.
[11] D. Liang, Y.-F. Liu, Z.-Y. Hao, H. Luo, Y. Wang, C.-L. Zhang, R.-Y. Chen, D.-Q. Yu, *Phytochem. Lett.* **2015**, *11*, 116–119. DOI: 10.1016/j.phytol.2014.12.006.
[12] S. Tsukamoto, B.-C. Cha, T. Ohta, *Tetrahedron* **2002**, *58*, 1667–1671. DOI: 10.1016/S0040-4020(02)00048-0.
[13] Y. Nakamura, *J. Chem. Soc., Chem. Commun.* **1988**, *7*, 477, DOI: 10.1039/C39880000477.
[14] F. Galindo, M. A. Miranda, *J. Photochem. Photobiol. A* **1998**, *113*, 155–161. DOI: 10.1016/S1010-6030(97)00330-4.
[15] G. K. Kole, J. J. Vittal, *J. Indian Chem. Soc.* **2022**, *99*, 100630. DOI: 10.1016/j.jics.2022.100630.
[16] C. McGowan, N. Leadbeater, in *Clean, Fast Organic Chemistry*, CEM Publishing: Matthews, NC, **2006**, p. 101.
[17] P. Elamathi, G. Chandrasekar, S. Muthuraman, M. K. Kolli, *Appl. Surf. Sci.* **2019**, *463*, 481–491. DOI: 10.1016/j.apsusc.2018.07.191.
[18] A. Elhampour, F. Nemati, *Org. Prep. Proced. Int.* **2017**, *49*, 443–458. DOI: 10.1080/00304948.2017.1374101.
[19] M. Golfmann, L. Glagow, A. Giakoumidakis, C. Golz, J. C. L. Walker, *Chem. Eur. J.* **2023**, *29*, 1–5. DOI: 10.1002/chem.202202373.
[20] H. Ziffer, A. Bax, R. J. Highet, B. Green, *J. Org. Chem.* **1988**, *53*, 895–896. DOI: 10.1021/jo00239a046.
[21] J. A. Juárez, M. A. Valenzuela-Zapata (Eds.) in *Cinética Química para sistemas homogéneos*. Instituto Politécnico Nacional. Tresguerras 27, México DF. **2002**. ISBN: 970–18-7985-6.
[22] L. Briones, J. M. Escola, *Educ. Chem. Eng.* **2019**, *26*, 41–47. DOI: 10.1016/j.ece.2018.10.003.
[23] J. Lelievre, P. G. Farrell, F. Terrier, *J. Chem. Soc., Perkin Trans. 2* **1986**, *2*, 333, DOI: 10.1039/P29860000333.
[24] T. L. Amyes, J. P. Richard, *J. Am. Chem. Soc.* **1996**, *118*, 3129–3141. DOI: 10.1021/ja953664v.
[25] C. K. Ingold: *Structure and Mechanism in Organic Chemistry*, 2nd ed., Cornell University Press, Ithaca, N. Y., London, **1969**, p. 457, 680. ISBN: 978–0713515688.
[26] D. M. Shin, D. G. Whitten, *J. Am. Chem. Soc.* **1998**, *110*, 5206–5208. DOI: 10.1021/ja00223a058.

Manuscript received: January 11, 2024